Differences and Similarities in the Reactivity of Peroxynitrite Anion and Peroxynitrous Acid with Ebselen. A Theoretical Study†

Djamaladdin G. Musaev*

Cherry L. Emerson Center for Scientific Computation and Department of Chemistry, Emory University, Atlanta, Georgia 30322

Kimihiko Hirao

Department of Applied Chemistry, School of Engineering, The University of Tokyo, Tokyo 113-8656, Japan

Received: October 28, 2002; In Final Form: January 6, 2003

The reaction mechanism of a model compound of ebselen, **2**, [1,2-benzisoselenazol-3(2*H*)-one], with peroxynitrous acid (HOONO) has been investigated using the density functional (B3LYP), coupled-cluster (CCSD(T)), and polarizable continuum model (PCM) methods, in conjunction with the 6-31G(d), 6-311G(d,p), 6-311+G(d,p), and 6-311+G(3df,2p) basis sets. It was shown that the B3LYP method is not reliable for studying the energetics and stability of the weakly bound $^{\bullet}$OH···ONO$^{\bullet}$ structure and may lead to the wrong conclusions. The CCSD(T) calculations with the 6-311+G(d,p) and 6-311+G(3df,2p) basis sets show that the disputed $^{\bullet}$OH···ONO$^{\bullet}$ structure is unlikely to exist in the gas phase. Including explicit solvent (water) molecules in the calculations resulted in a complete cleavage of the weak interaction between the $^{\bullet}$OH and ONO$^{\bullet}$ radicals in $^{\bullet}$OH···ONO$^{\bullet}$. The reaction of **2** + HOONO → **2**−O + HONO was found to be exothermic in the gas phase by 25.3 (24.9) kcal/mol and may proceed via two different pathways: stepwise and concerted. The concerted mechanism, which proceeds via the O−O bond cleavage transition state, was found to be more favorable at the enthalpy level. However, including an entropy correction makes the stepwise mechanism more favorable, which proceeds through the O−O bond homolysis in *cis*-HOONO. Even in solution, the reaction of compound **2** (and ebselen) with HOONO prefers to proceed via the concerted mechanism. A comparison of the reaction mechanisms of **2** with HOONO and $ONOO^-$ (as reported previously (*J. Am. Chem. Soc.*, in press)[22]) shows that the reaction of **2** (and ebselen) with HOONO should be slower than that with $ONOO^-$ in both the gas phase and in solution. We have shown that the observed (*FEBS Lett.* **1996**, *398*, 179)[20] lower yield of selenoxide at high pH values is partially due to the large O−O bond cleavage barrier for HOONO versus $ONOO^-$. Our analysis shows that reaction of **2** with $ONOO^-$ is a two-electron oxidation process and occurs via heterolytic O−O bond cleavage, whereas the reaction of **2** with HOONO is a one-electron oxidation process and occurs via homolytic O−O bond cleavage.

I. Introduction

The peroxynitrite anion ($ONOO^-$, PN) formed by the direct and rapid combination of nitric oxide (NO) and superoxide anion (O_2^-).

$$NO + O_2^- \leftrightarrow ONOO^-$$

is stable in alkaline solution[1] but quickly isomerizes to its nitrate form, or undergoes homolysis to yield $^{\bullet}$OH and $^{\bullet}NO_2$ radical pairs (or an $^{\bullet}OH\cdots{}^{\bullet}NO_2$ "cage-radical") upon protonation.[2,3] Peroxynitrite† and the related $^{\bullet}$OH, $^{\bullet}NO_2$, and $^{\bullet}CO_3^-$ (formed from the reaction of $ONOO^-$ with CO_2) radicals rapidly react with numerous bio-molecules, including proteins (via the nitration of tyrosine and tryptophan), lipids (via peroxidation), DNA, and aromatic compounds.[4−12] The high reactivity of peroxynitrite (or related radicals) with biological targets, combined with their high mobility (even in the presence of biological membranes), implicates it in many diseases states, including heart disease, cancer, and apoptotic cell death in leukemia cells, aortic smooth muscle cells, and neural cells. Therefore, it is quite important to search for drugs that can intercept the powerful oxidizing and nitrating agent, peroxynitrite, and thus, detoxify it. In this respect, elucidation of the detailed mechanisms of the reaction of $ONOO^-$ and peroxynitrous acid (HOONO) with numerous potentially useful organic and organometallic antioxidants becomes extremely important. The better understanding of the roles of the electronic, steric, and solvent effects in these reactions will enhance our ability to search for more effective drugs against peroxynitrite.

In the literature, it has been shown that a series of water-soluble Fe(III) porphyrin complexes,[13,14] heme-containing proteins,[15] selenoproteins,[16] and synthetic organo-selenium compounds[17] (e.g., ebselen, [2-phenyl-1,2-benzisoselenazol-3(2*H*)-one[18]] and organo-sulfur compounds (e.g., methionine)[19] can intercept and/or catalyze the decomposition and isomerization of peroxynitrite. Among these species, ebselen is one of the promising candidates[17,18] (see Scheme 1). It has been shown that ebselen reacts with $ONOO^-$ with a rate constant of $2.0 \times 10^6\ M^{-1}\ s^{-1}$ in alkaline pH solutions via an oxygen atom

† Peroxynitrite is used to refer to the peroxynitrite anion, $O{=}NOO^-$, and peroxynitrous acid, ONOOH, unless otherwise indicated. The IUPAC recommended names are oxoperoxonitrate(−1) and hydrogen oxoperoxonitrate, respectively. The abbreviation PN is also used to refer to the peroxynitrite anion.

10.1021/jp027324p CCC: $25.00
Published on Web 02/13/2003

SCHEME 1: Schematic Presentation of the Se Compounds Used in Our Previous Paper[22]

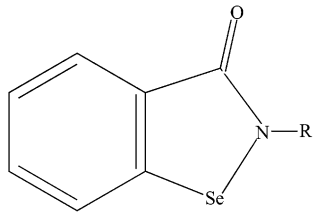

R=Ph	-	**1, Ebselen**	$R=OSiH_3$	-	**5**
R=H	-	**2**	R=OH	-	**6**
R=Me	-	**3**	$R=NH_2$	-	**7**
$R=CF_3$	-	**4**			

transfer mechanism to produce the selenoxide and nitrite.[20,21] This reaction also occurs at acidic pH, where the peroxynitrite anion is predominantly protonated to form peroxynitrous acid (HOONO), and produces the selenoxide as the main product. However, in solutions with high pH's, a lower yield of selenoxide is observed.[20] This can be explained in terms of either the larger O−O bond cleavage barrier for HOONO versus $ONOO^-$, or the existence of competing ebselen oxidation reactions, such as the spontaneous decay of HOONO, and the pH-dependent formation of byproducts, or a combination of all of these. However, to the best of our knowledge, the answers to these questions still need to be elucidated. Furthermore, current experiments[20,21] have not provided any information on the geometries and energetics of the reactants, the expected intermediates, the transition states, or on the products. The roles of the electronic, steric, and solvent effects on the reaction of ebselen with $ONOO^-$ and HOONO also need to be elucidated. For solving these questions the quantum chemical calculations on the reaction mechanisms of ebselen with $ONOO^-$ and HOONO could be extremely useful.

In a previous paper[22] we carried out detailed studies on the reaction mechanism of ebselen, **1**, and its derivatives, **2**−**7** (see Scheme 1), with the peroxynitrite anion. Briefly, we shown that the reaction of **2** (a model of ebselen) with $ONOO^-$ (PN) proceeds via the pathway: **2** + PN → **2**−PN → **2**−TS1 (O−O activ.) → **2**−(O)(NO_2^-) → **2**−O + NO_2^-. In the gas phase, the rate-determining Gibbs free energy barrier of (14.8) kcal/mol corresponds to the NO_2^- dissociation step (throughout this paper, the Gibbs free energy will be given in parentheses, and the total energy values will be given without parentheses). The direct products of this reaction are the NO_2^- anion and selenoxide. The second possible process, the NO_3^- formation starting from the **2**−(O)(NO_2^-) complex, requires (7.9) kcal/mol more energy than NO_2^- dissociation from **2**−(O)(NO_2^-) and so is unlikely to energetically compete with the latter. Thus, in the gas phase, peroxynitrite → nitrate isomerization catalyzed by complex **2** is unlikely to occur. Furthermore, the calculated Gibbs free energy difference, Δ, between the rate-determining steps of the NO_2^- dissociation and NO_3^- formation processes, increases with the increasing electron-withdrawing ability of the R group, i.e., H(2.6) ≈ CH_3(2.0) < C_6H_5(8.1) < CF_3(14.8). (Here, we show the Δ*E* values, which do not include the zero-point energy and entropy corrections). We found that the energy for the NO_3^- formation process is slightly (3.3 kcal/mol after including the zero-point energy and entropy corrections) more favorable than the NO_2^- dissociation process for compound **4**, which possesses the strongest electron-withdrawing group, R = CF_3. Therefore, we predicted that compound **4** would be a good catalyst for the peroxynitrite ↔ nitrite isomerization in the gas phase. Another promising catalyst for the peroxynitrite ↔ nitrite isomerization in the gas phase is predicted to be complex **6**, with R = OH. Also, we have shown that the Se−N^2 bond of compound **2** is extremely flexible, undergoing significant changes during the reaction, and so facilitating the entire reaction. We predicted that the ebselen derivatives with nonexistent (or weak) Se−N^2 bonds would be extremely active for $ONOO^-$ coordination and the O−O bond cleavage, as well as for nitrate formation, whereas the ebselen derivatives with a strong Se−N^2 bond are expected to be extremely useful for the NO_2^- dissociation step.

However, the inclusion of solvent effects changes the rate-determining step of reaction **2** with PN from the NO_2^- dissociation to the O−O cleavage step, which is calculated to occur with energy barriers of 8.3 (13.9), 7.8 (8.4), 7.8 (8.4), and 7.6 (8.2) kcal/mol in water, dichloromethane, benzene, and cyclohexane, respectively. Furthermore, solvent effects make the peroxynitrite ↔ nitrate isomerization process practically impossible, even for complex **4**, with R = CF_3. Therefore, the direct products of the reaction of **1**−**7** with PN are predicted to be nitrite and selenoxide molecules. This conclusion is in agreement with available experiment data.[20,21]

The present work is a continuation of our previous studies and is concerned with studies on the mechanism of, and factors affecting, the reaction of ebselen with peroxynitrous acid. We believe that studies on the reaction mechanism of ebselen with HOONO, and the comparison the obtained results with our previous[22] results for $ONOO^-$, will allow us to elucidate the differences and/or similarities in the O−O bond cleavage of $ONOO^-$ and HOONO by ebselen. Previously,[22] complex **2**, [1,2-benzisoselenazol-3(2*H*)-one] was found to be a good model for ebselen. Therefore, below, we studied the reaction of the model complex **2** with HOONO, in a manner similar to that previously reported for $ONOO^-$.[22]

II. Calculation Procedures

All calculations were performed using the quantum chemical package GAUSSIAN-98.[23] The geometries, vibrational frequencies, and energetics of all the reactants, intermediates, transition states, and products were calculated using hybrid density functional theory employing the B3LYP method.[24] In these calculations, we used two types of basis sets: 6-311G(d,p) and 6-311+G(d,p). Our benchmark studies[22] on the geometries of several intermediates and reactants of the reaction of **2** with $ONOO^-$ at the B3LYP/6-311G(d,p) and B3LYP/6-311+G(d,p) levels, show that a diffuse function is not important for the geometry calculations. Differences in the calculated geometrical parameters are negligible upon going from the B3LYP/6-311G(d,p) to the B3LYP/6-311+G(d,p) level. Therefore, we, mainly, report on the B3LYP/6-311G(d,p) calculations alone, for the optimized geometries and vibrational frequencies of the reaction of **2** with HOONO. Our studies[22] have also revealed that the role of a diffuse function can be crucial in the calculations of the relative energies. Therefore, we will discuss only the B3LYP/6-311+G(d,p) energetics (where the total energy-based values will be given without parentheses, and the Gibbs free energies will be presented in parentheses) calculated at the B3LYP/6-311G(d,p) optimized geometries for all located structures (below, this approach is denoted as B3LYP/6-311+G(d,p)//B3LYP/6-311G(d,p)), unless otherwise stated. Previous studies[25,26] on the structure and stability of *cis*- and *trans*-HOONO, as well as the transition state that separates them, show that the B3LYP method, and more sophisticated approaches, such as CCSD(T), G2 and CBS-Q using the 6-311+G(d,p) basis sets are in very close agreement. Meantime, the extensive studies of the reactivity of HOONO with alkenes, sulfides, amines, and phosphines by Bach and co-workers[27] at

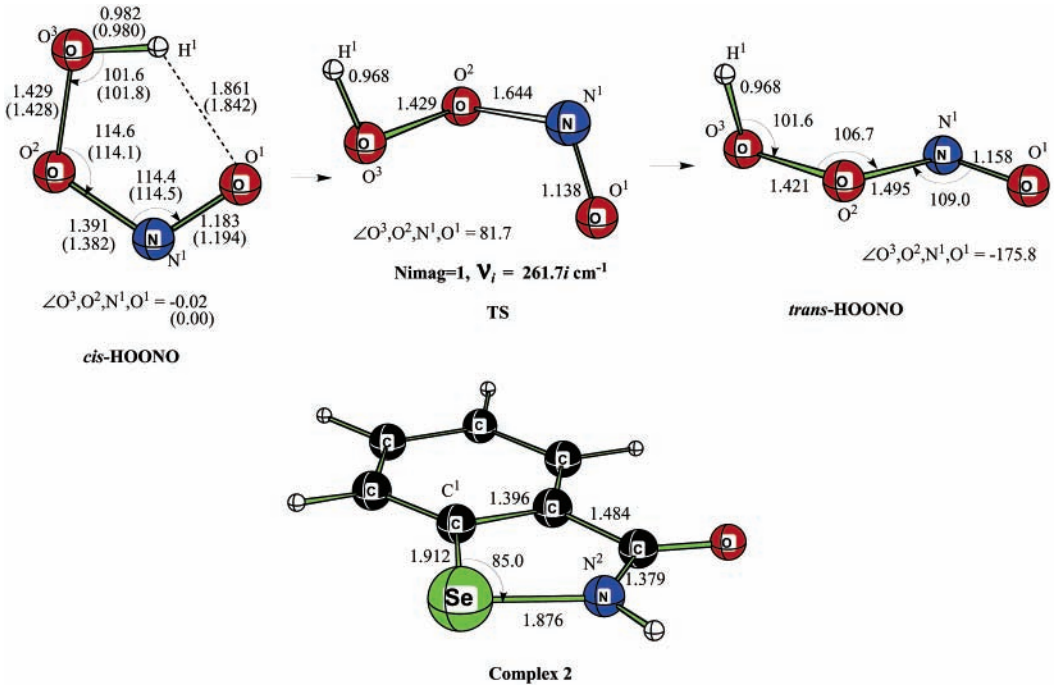

Figure 1. B3LYP/6-311G(d,p) calculated important geometrical parameters (distances in Å, angles in deg) of the reaction of compound **2** with HOONO. Numbers given in the parenthesis were calculated at the MP2(full)/6-311+G(d,p) level.

various levels of theory (e.g., B3LYP, MP2, MP4, CISD, QCISD, and QCISD(T)) indicate that the B3LYP method underestimates the calculated O−O bond activation barriers by a few kcal/mol compared to the QCISD(T) method. Because our major task is to compare the reactivity of compound **2** with HOONO and $ONOO^-$ by investigating them at the same (B3LYP/6-311+G(d,p)) level of theory, we believe that any underestimation of the O−O bond cleavage barriers by the B3LYP method will not affect our conclusions.

Furthermore, in our studies on the structure and stability of the actively debated hydrogen-bound $^{\bullet}OH\cdots ONO^{\bullet}$ structure, we have used both the B3LYP, MP2(full), and the more sophisticated CCSD(T) methods with different quality basis sets including very large one, 6-311+G(3df,2p). The details of these calculations will be presented in section III.

To analyze the effect of the solvent on the reaction mechanism of **2** with HOONO, we have performed single point Polarizable Continuum Model[28] calculations at the B3LYP/6-311G(d,p) level optimized geometries, PCM-B3LYP/6-311+G(d,p). The solvents we choose are water, dichloromethane, benzene, and cyclohexane. The default dielectric constants of these solvents were taken from the Gaussian-98 program.[23]

This paper is organized as follows. In section III, we discuss the mechanism of the reaction of compound **2** with HOONO in the gas phase and compare our results with available theoretical and experiment data, whereas in section IV, we elucidate the role of solvent effects. Section V is devoted to a comparison of the reaction mechanisms of compound **2** with $ONOO^-$ and HOONO, followed by our conclusions.

III. Results and Discussion

We begin our discussions with the structure, stability, and reactivity of the HOONO molecule. The calculated geometries and energetics of HOONO are given in Figure 1 and Table 1, respectively.

Compound **2** was discussed in detail in a previous paper,[22] and we will not repeat those discussions here. However, to facilitate our analysis of the mechanism of reaction **2** with HOONO, we have included the energies, structure, and geometries of **2** in Figure 1 and Table 1.

TABLE 1: Calculated Relative Energies (kcal/mol) of the Reactants, Intermediates, Transition States, and Products of the Reaction of 2 with HOONO

	6-311G(d,p)				6-311+G(d,p)	
structures	ΔE	ΔE + ZPC	ΔG	$\Delta\Delta$	ΔE	ΔG
HOONO						
cis	0.0	0.0	0.0	0.0	0.0	0.0
TS	15.1	14.3	14.2	0.9	13.4	12.5
trans	3.6	3.3	3.1	0.5	2.1	1.6
HONO						
cis	0.0	0.0	0.0	0.0	0.0	0.0
TS	13.3	12.0	11.9	1.4	11.8	10.4
trans	0.3	0.3	0.3	0.0	−1.1	−1.1
2 + *cis*-HOONO	0.0	0.0	0.0	0.0	0.0	0.0
2−*cis*-HOONO-with_OH	−2.9	−2.7	5.6	8.5	−2.1	6.4
2−*cis*-HOONO-with_N	−1.3	−0.9	6.8	8.1	−0.8	7.3
2−*trans*-HOONO	−0.2	0.1	9.9	10.1	−1.0	9.1
2−TS1 (O−O activ.)	0.5	0.3	11.0	10.5	0.9	11.4
2−$(OH)(NO_2)$	−34.8	−33.5	−21.1	13.7	−34.8	−21.1
2−TS2 (H-transfer)	−32.3	−33.5	−20.8	11.5	−32.3	−20.8
2−O(HONO)	−35.3	−34.3	−23.2	12.1	−35.8	−23.7
2−O + HONO	−23.0	−23.1	−22.6	0.4	−25.3	−24.9
2−OH + NO_2	−10.4	−11.2	−11.1	0.7	−12.1	-12.8

As mentioned above, peroxynitrous acid has been the subject of numerous previous theoretical studies.[25,27,29,30] Briefly, it has been shown that *cis*-HOONO is more stable than *trans*-HOONO by 1−2 kcal/mol and that the barrier separating these isomers corresponds to the torsion around the HO−ONO bond, which is found to have an energy of about 12 kcal/mol. The data presented in Figure 1 and Table 1 are consistent with those reported previously.[25,29] Indeed, we found that *cis*-HOONO is more stable than *trans*-HOONO by 1.6 kcal/mol and separated from the latter by a 12.5 kcal/mol energy barrier. The torsion angle at the transition state was calculated to be 81.7°, which is very close to that reported previously.[25]

It has been shown that the protonation of $ONOO^-$ catalyzes the rearrangement of peroxynitrite to nitrate.[2,3] The experimental activation enthalpy and Gibbs free activation energy of this

TABLE 2: Calculated Energies (Relative to *cis*-HOONO, in kcal/mol) of the OH···ONO Structure and OH + ONO Dissociation Limit at the Various Levels of Theory

		•OH···ONO•				•OH + ONO•			
method	basis sets	ΔE	ΔE + ZPC	ΔG	$\Delta\Delta(\Delta G - \Delta E)$	ΔE	ΔE + ZPC	ΔG	$\Delta\Delta(\Delta G - \Delta E)$
B3LYP	6-31G(d)	20.0	16.9	14.7	−5.3	22.5	18.4	9.5	−13.0
	6-311G(d,p)	8.1	8.9	6.0	−2.1	18.4	14.4	5.5	−12.9
	6-311+G(d,p)	8.8	6.0	2.0	−6.8	14.8	11.0	2.2	−12.6
	6-311+G(3df,2p)	16.1	13.1	9.2	−6.9	17.3	13.3	3.9	−13.4
CCSD(%)[a]	6-311+G(d,p)	13.7	[11.9][b]	[7.9]		14.9	[11.0]	[2.2]	
	6-311+G(3df,2p)	19.1	[16.1]	[12.2]		20.1	[16.1]	[6.7]	
MP2(full)	6-311+G(d,p)	10.1				11.6			
CCSD(T)[c]	6-311+G(d,p)	13.4				15.0			

[a] These CCSD(T) results were obtained at the B3LYP optimized geometries using the same basis sets. [b] In brackets were given the estimated values using the ZPC and ΔΔ calculated at the B3LYP/same basis sets level. [c] These CCSD(T) data were obtained at the MP2(full)/6-311+G(d,p) optimized geometries.

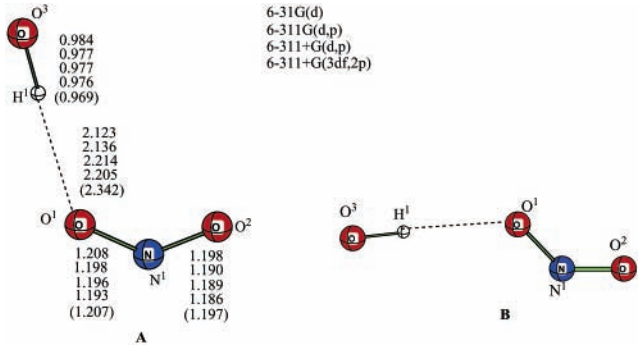

Figure 2. Presentation of the two isomers (**A** and **B**) of •OH···ONO• structure reported in ref 35. In the present paper we study only isomer **A**, the geometrical parameters (in Å) of which, calculated at the B3LYP level with various basis sets, are presented in this figure. Numbers given in the parenthesis were calculated at the MP2(full)/6-311+G(d,p) level.

process were found to be 18 ± 1 and 17 ± 1 kcal/mol in solution.[31,32] In the literature,[33] two distinct mechanisms of peroxynitrite to nitrate isomerization are actively debated: (1) the homolysis of the O−O bond in HOONO to yield HO• and ONO• radicals or a weakly bound •OH···ONO• radical pair and (2) a unimolecular concerted pathway. Numerous theoretical studies[33,34] have been performed at different levels of theory and have demonstrated that a concerted barrier for HOONO → HNO_3 isomerization is very high, at 47−60 kcal/mol, and cannot contribute to the peroxynitrite-to-nitrate isomerization. Therefore, the most likely pathway for HOONO → HNO_3 isomerization is the O−O bond homolysis, which may proceed with and/or without the formation of a weakly bound •OH···ONO• intermediate. In the gas phase, the enthalpy and Gibbs free energies of the O−O bond dissociation in HOONO are calculated to be 20−22 and (9−10) kcal/mol at the different levels of theory.[33,35] Recently, from the B3LYP/6-31G* calculations, Houk and co-workers[35] have predicted the existence of a weakly bound •OH···ONO• structure, which was suggested as an attractive structure for the potent oxidizing intermediate HOONO*, suggested by experimentalists.[31] They have predicted two distinct isomers, **A** and **B** for •OH···ONO• (see Figure 2), which lie 1.9 and 2.5 kcal/mol lower than the dissociation limit of •OH + $•NO_2$. The predicted Gibbs free energy of the reaction •OH···ONO• → HOONO is 15.6 and 15.0 kcal/mol for structures **A** and **B**, respectively. Because the existence of the weakly bound •OH···ONO• structure is one of the actively debated issues in the peroxynitrite-related literature, below we will discuss this problem in more detail.

O−O Bond Homolysis in Peroxynitrous Acid, and the Possibility of the Existence of the Weakly Bound •OH···ONO• Structure. Initially, we performed B3LYP/6-31G(d) calculations on the *cis*-HOONO and •OH···ONO• (isomer **A**) structures, as well as on the •OH+ONO• dissociation limit. As can be seen in Table 2, where we present the obtained energetics at the B3LYP/6-31G(d) level, the Gibbs free energy of the reaction •OH···ONO• → *cis*-HOONO is 14.7 kcal/mol, which is consistent with the 15.0 kcal/mol reported by Houk and coworkers[35] by using the same level of theory.

The •OH···ONO• structure lies 1.5 kcal/mol lower than the •OH+ONO• dissociation limit at the ΔE + ZPC level. However, the inclusion of an entropy correction lowers the stability of the •OH···ONO• structure by 5.2 kcal/mol versus the •OH···ONO• dissociation limit. In other words, our calculations show that at the Gibbs free energy level, the •OH+ONO• structure is not stable relative to the •OH+ONO• dissociation limit in the gas phase.

To clarify the method and basis set effects on the structure and stability of *cis*-HOONO and •OH···ONO• (isomer **A**) and on the •OH+ONO• dissociation limit, we performed extensive calculations using the B3LYP, MP2 and the more sophisticated CCSD(T) methods. In these calculations, we used higher quality basis sets, such as the 6-311G(d,p), 6-311+G(d,p), and 6-311+G(3df,2p). The results obtained are presented in Figures 1 and 2 and in Table 2.

The B3LYP data presented in Figure 2 shows that the important geometrical parameters of the •OH···ONO• structure are not basis set dependent. The maximum difference was found to be along the O^1-H^1 bond distance, which was elongated by 0.07−0.09 Å upon moving to the large 6-311+G(d,p) and 6-311+G(3df,2p) basis sets. However, in the hydrogen-bonded systems, like •OH···ONO•, the qualitative accuracy often requires more accurate treatment of electron correlation, dispersion and van der Waals interactions. Unfortunately, as it previously was demonstrated,[36] the B3LYP method used in the optimization geometries of the *cis*-HOONO and •OH···ONO• structures, may not properly describe these interactions. Previously,[36] the MP2 method in conjunction with the large basis sets was recommended to be an optimal approach for these types of studies. Therefore, to evaluate the accuracy of the B3LYP optimized geometries of the *cis*-HOONO and •OH···ONO• structures we have performed the MP2(full)/6-311+G(d,p) optimization of the geometries of these systems. The obtained geometries are given in the Figures 1 and 2. As seen from these data, B3LYP/6-311+G(d,p) and MP2(full)/6-311+G(d,p) optimized geometries are almost identical (within ca. 0.01 Å) with the exception of the O^1-H^1 bond distance: in the *cis*-HOONO and •OH···ONO• structures the MP2 optimized O^1-H^1 bond distance is 0.019 Å shorter and 0.128 Å longer than its B3LYP values, respectively. In any case, these two methods provide very close results. Similar conclusion were made by Bach and

co-workers[27] on the optimization of the geometries of *cis*-HOONO at the B3LYP, MP2, QCISD and QCISD(T) levels.

However, the calculated B3LYP energetics show a strong oscillation upon using the improved basis sets. Indeed, the calculated energy difference (using ΔE + ZPC values) between the •OH+ONO• structure and the •OH···ONO• dissociation limit is found to be 1.5, 5.3. 5.0, and 0.2 kcal/mol at the 6-31G(d), 6-311G(d,p), 6-311+G(d,p), and 6-311+G(3df,2p) basis sets, respectively. In other words, for the best and worst basis sets used in this paper, the •OH···ONO• structure is only slightly more stable than the dissociation limit. Using the medium quality basis sets, the stability of the •OH···ONO• structure is significantly increased. The inclusion of the entropy correction makes the •OH···ONO• structure either highly unstable (by 5.2 and 5.3 kcal/mol for the 6-31G(d) and 6-311+G(3df,2p) basis sets, respectively) or only slightly stable (by 0.5 and 0.2 kcal/mol for the 6-311G(d,p) and 6-311+G(d,p) basis sets, respectively). Furthermore, the calculated energy difference between the *cis*-HOONO and •OH···ONO• structures are 16.9, 8.9, 6.0, and 13.1 kcal/mol using the ΔE + ZPC values, and 14.7, 6.0, 2.0, and 9.2 kcal/mol using the Gibbs free energy values, for the 6-31G(d), 6-311G(d,p), 6-311+G(d,p), and 6-311+G(3df,2p) basis sets, respectively. Thus, the smallest basis set provides better agreement with the experimentally measured enthalpy and Gibbs free energy of activation of peroxynitrite-to-nitrate isomerization in solution, of 18 ± 1 and 17 ± 1 kcal/mol, respectively.[32] *However, the general conclusion from the data is that the B3LYP method provides an inconclusive picture of the energetics and the stability of the weakly bound •OH···ONO• structure.*

The data presented in the Table 2 shows that the MP2(full) method provides the same conclusion as the B3LYP method: the •OH···ONO• structure lies lower in energy (ΔE values) than the •OH + ONO• dissociation limit. However, the energy difference (ΔE) between the •OH···ONO• structure and the •OH + ONO• dissociation limit is much smaller (1.5 kcal/mol) in MP2 level than in the B3LYP level (6.0 kcal/mol). In the other words, the including more electron correlation effects reduces the energy difference between the •OH···ONO• structure and the •OH + ONO• dissociation limit.

In the next step, we have performed two sets of CCSD(T) calculations to include much more electron correlation effects in the calculations compared to the MP2(full) method. The first set of CCSD(T) calculations uses the largest basis sets, 6-311+G(d,p) and 6-311+G(3df,2p), and the B3LYP/6-311+G(d,p) and B3LYP/6-311+G(3df,2p) optimized geometries, respectively, whereas the second set of CCSD(T) calculations uses the 6-311+G(d,p) basis set and MP2(full)/6-311+G(d,p) optimized geometries. The obtained results are shown in Table 2.

At first, these calculations show that the CCSD(T) method using 6-311+G(d,p) basis sets, and B3LYP/6-311+G(d,p) and MP2(full)/6-311+G(d,p) optimized geometries provide extremely close results. Indeed, the •OH···ONO• structure is calculated (ΔE values) to be 13.7 and 13.4 kcal/mol higher than *cis*-HOONO using the B3LYP/6-311+G(d,p) and MP2(full)/6-311+G(d,p) optimized geometries, respectively. The •OH + ONO• dissociation limit is found to lie only 14.9 and 15.0 kcal/mol higher than *cis*-HOONO using the B3LYP/6-311+G(d,p) and MP2(full)/6-311+G(d,p) optimized geometries, respectively. In the other words, these calculations, once again, demonstrate that B3LYP and MP2(full) methods provide very close geometries for *cis*-HOONO, •OH···ONO• structures and related species.

Meantime, our best calculations at the CCSD(T)/6-311+G(3df,2p) level using B3LYP/6-311+G(3df,2p) geometries show that the •OH···ONO• structure lies 19.1, 16.1, and 12.2 kcal/mol higher than *cis*-HOONO, at the ΔE, ΔE + ZPC, and ΔG levels, respectively, whereas the •OH+ONO• dissociation limit was calculated to be 20.1, 16.1, and 6.7 kcal/mol higher than the *cis*-HOONO structure at the ΔE, ΔE + ZPC, and ΔG levels, respectively. In other words, the •OH···ONO• structure is not thermodynamically stable relative to the •OH+ONO• dissociation limit. The O−O bond dissociation energy of 16.1 kcal/mol (ΔE + ZPC value) calculated at the CCSD(T)/6-311+G(3df,2p) level is in very good agreement with the 18 ± 1 kcal/mol experimental enthalpy of activation of peroxynitrite-to-nitrate isomerization in solution.[31] However, the calculated Gibbs free energy values for the reactions, *cis*-HOONO → •OH···ONO• and *cis*-HOONO → •OH + ONO• of 12.2 and 6.7 kcal/mol, respectively, are significantly smaller than the experimental Gibbs free energy of activation of 17 ± 1 kcal/mol for the peroxynitrite-to-nitrate isomerization in solution.[32] However, one should note that we cannot compare the calculated Gibbs free energy in the gas phase with its experimental value in solution, because in solution, the entropy effect is expected to be much smaller than in the gas phase.

Thus, our CCSD(T) calculations (after including the zero-point energy (ZPC) and entropy corrections) *show that the •OH···ONO• structure most likely does not exist in the gas phase.*

It is noteworthy that the performed T1 test during the CCSD(T) calculations shows that the wave functions of both the *cis*-HOONO and the •OH···ONO• structures have, mainly, single determinant characters: their T1 diagnostic values are calculated to be 0.0141 and 0.0219 at the CCSD(T)/6-311+G(d,p) level, respectively. Therefore, it is expected that the application of multi-determinant based methods such as MCSCF, CASSCF, etc. to the study of these structures will not change the conclusions made on the basis of the single-determinant approaches such as B3LYP, MP2, and CCSD(T). Similarly, the comparison of the MCSCF results of Krauss[37] for peroxynitrite anion with those obtained at the single determinant levels (B3LYP, MP2, QCISD(T), etc.)[25,30] show that the multi-determinant character of $ONOO^-$ (and most likely of HOONO) is negligible.

To elucidate the role of the solvent molecules on the structure and stability of •OH···ONO•, we explicitly included solvent molecules in our calculations. The B3LYP/6-311+G(d,p) optimization of the geometrical structures of the $(H_2O)_n$(•OH···ONO•) complexes (with n = 1 and 2) shows that the weak interaction between the •OH and ONO• radicals completely disappears on increasing the number of surrounding water molecules (see Figure 3).

For n = 1, there still exists a weak interaction between •OH and ONO• radicals with an H^1-O^1 bond distance of 2.241 Å, whereas for n = 2, this interaction completely vanishes, and the •OH radical becomes solvated by water molecules. In other words, *these data clearly demonstrate that in water the weak •OH−ONO• interaction in •OH···ONO• completely vanishes, and the •OH and ONO• radicals are surrounded by solvent molecules. Thus, in solution, the reactivity of HOONO with antioxidants, if it proceeds via an O−O homolysis mechanism, should resemble that of a solvated •OH radical, at least in polar solvents, such as water.*

Reactivity of HOONO with Complex 2. The reactivity of peroxynitrous acid with numerous antioxidants has been the subject of many previous theoretical[27,33,35] and experimental[38] studies. In general, it was shown that peroxynitrous acid acts

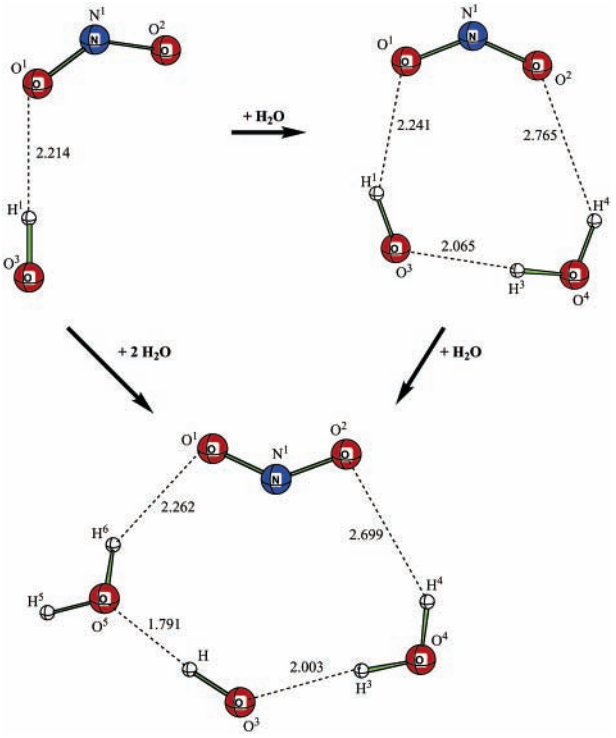

Figure 3. B3LYP/6-311+G(d,p) calculated structures and important distances (in Å) of the $(H_2O)_n$(•OH···ONO•) complexes, where $n = 0$, 1, and 2.

as both a one- and a two-electron oxidant. One-electron oxidation by HOONO proceeds via either direct electron transfer to peroxynitrous acid, or via O−O bond homolysis, leading to a hydroxyl radical or to hydrogen-bound radical pairs, accompanied by electron transfer. As an example, the one-electron oxidation of methionine by HOONO leads to the formation of ethylene.[39] Two-electron oxidation is an oxygen transfer process. Note that the reactivity of peroxynitrous acid with amines, sulfides, alkenes, and phosphines has been discussed at different levels of theory, including the B3LYP level.[27,33,35]

In the present paper we studied the reaction mechanism of the Se-containing compound **2** with HOONO. As we stated above, the reaction of compound **2** with HOONO may proceed via two different pathways: stepwise and concerted. The concerted pathway starts with the O−O bond cleavage via one-electron oxidation by HOONO, whereas the first step of the stepwise pathway corresponds to the O−O bond homolysis in *cis*-HOONO leading to the formation of HO• and ONO• radical pairs. Because the O−O bond homolysis in *cis*-HOONO was detailed discussed above, below we describe the stepwise pathway of the reaction of **2** with HOONO. The first possible intermediate of the reaction of **2** with HOONO is expected to be a **2**−HOONO molecular complex.

2−HOONO Complex. As discussed above, HOONO has two different isomers: cis and trans. Therefore, the **2**−HOONO complex could have various isomeric forms. We have located three different **2**−HOONO isomers: **2**−*cis*-HOONO_with_OH, **2**−*cis*-HOONO_with_N, and **2**−*trans*-HOONO (see Figure 4).

The first two isomers correspond to the coordination of the most energetically stable cis form of HOONO to compound **2**, whereas the third isomer is the result of the coordination of *trans*-HOONO to **2**. As seen in Figure 4, in isomer **2**−*cis*-HOONO_with_OH the *cis*-HOONO is coordinated to compound **2** by its most negatively charged O^3 atom, whereas in **2**−*cis*-HOONO_with_N, *cis*-HOONO is coordinated by its N^1 center. In **2**−*trans*-HOONO, the *trans*-HOONO is coordinated to **2** by its H^1 end. The main geometric parameters of HOONO and compound **2** in the **2**−HOONO complex are almost the same as those of the free reactants (for more information, see Table S1 of the Supporting Information Available). The calculated Se−O^3, Se−N^1, and Se−H^1 bond distances are 3.001, 3.369, and 2.510 Å for isomers **2**−*cis*-HOONO_with_OH, **2**−*cis*-HOONO_with_N, and **2**−*trans*-HOONO, respectively. In addition, the weak hydrogen bonds exist between the coordinated atomic centers of the *cis*-HOONO fragment and the H^2 atom of the phenyl group. The calculated O^3−H^2 and N^1−H^2 bond distances are 2.746 and 2.893 Å, respectively, for **2**−*cis*-HOONO_with_OH and **2**−*cis*-HOONO_with_N.

The discussed geometric parameters are consistent with the existence of an extremely weak interaction between the HOONO molecule and compound **2**. As can be seen in Table 1, the reaction of *cis*-HOONO and **2** is exothermic (from the ΔE values) by 2.1 and 0.8 kcal/mol for the formation of the **2**−*cis*-HOONO_with_OH and **2**−*cis*-HOONO_with_N isomers, respectively. The reaction of ***trans*-HOONO + 2 → 2**−*trans*-HOONO is slightly more exothermic, at 3.1 kcal/mol. However, the inclusion of entropy and zero-point energy corrections makes the formation of the **2**−HOONO complex an endothermic process by (6.4), (7.3), and (10.7) kcal/mol (relative to *trans*-HOONO) for the **2**−*cis*-HOONO_with_OH, **2**−*cis*-HOONO_with_N, and **2**−*trans*-HOONO isomers, respectively. Thus, it is most likely that the reaction of HOONO and compound **2** does not form a **2**−HOONO intermediate in the gas phase. Therefore, the first step of the reaction of HOONO with **2** in the gas phase is expected to be a HO−ONO bond cleavage.

Transition States for HO−ONO Bond Cleavage. The transition state, **2**−TS1(O−O activ.), corresponding to the O^3−O^2 bond cleavage of *cis*-HOONO by compound **2**, is shown in Figure 4. The nature of this transition state was positively characterized by performing normal-mode analysis: it is a real transition state with only one imaginary frequency of 259.9i cm^{-1}, corresponding to the O^3−O^2 activation process. The intrinsic reaction coordinate[40] (IRC) calculations that were performed show that this transition state connects the **2**−*cis*-HOONO_with_OH complex with the O^3−O^2 bond cleavage product, **2**−(OH)(NO_2), shown in Figure 4.

As can be seen in Figure 4, in **2**−TS1(O−O activ.), the broken O^3−O^2 bond distance is elongated by 0.289 Å, whereas the formed Se−O^3 and N^1−O^2 bond distances are shortened by 0.614 and 0.119 Å, respectively, when compared to the corresponding pre-reaction complex **2**−*cis*-HOONO_with_OH. All these geometrical changes are consistent with the nature of this transition state, where O^3−O^2 bond cleavage and Se−O^3 and N^1═O^2 double bond formations occur. One should note that during the process the strong Se−O^3 bond is formed, whereas the Se−C^1 and Se−N^2 bonds are slightly elongated.

The enthalpy and Gibbs free energy activation barriers were calculated to be 0.9 and (11.4) kcal/mol, respectively. Note that because the pre-reaction complex **2**−HOONO does not exist at the Gibbs free energy level, the barriers were calculated relative to the reactants, *cis*-HOONO and **2**.

We did not calculate the O^3−O^2 bond activation transition state for the energetically less favorable trans isomer of HOONO. We do not expect this transition state to be significantly different, either energetically or geometrically, from that of **2**−TS1(O−O activ.) discussed above, and it can therefore be ignored.

Products of O−O Bond Cleavage. As stated above, overcoming the transition state of **2**−TS1(O−O activ.)**,** leads

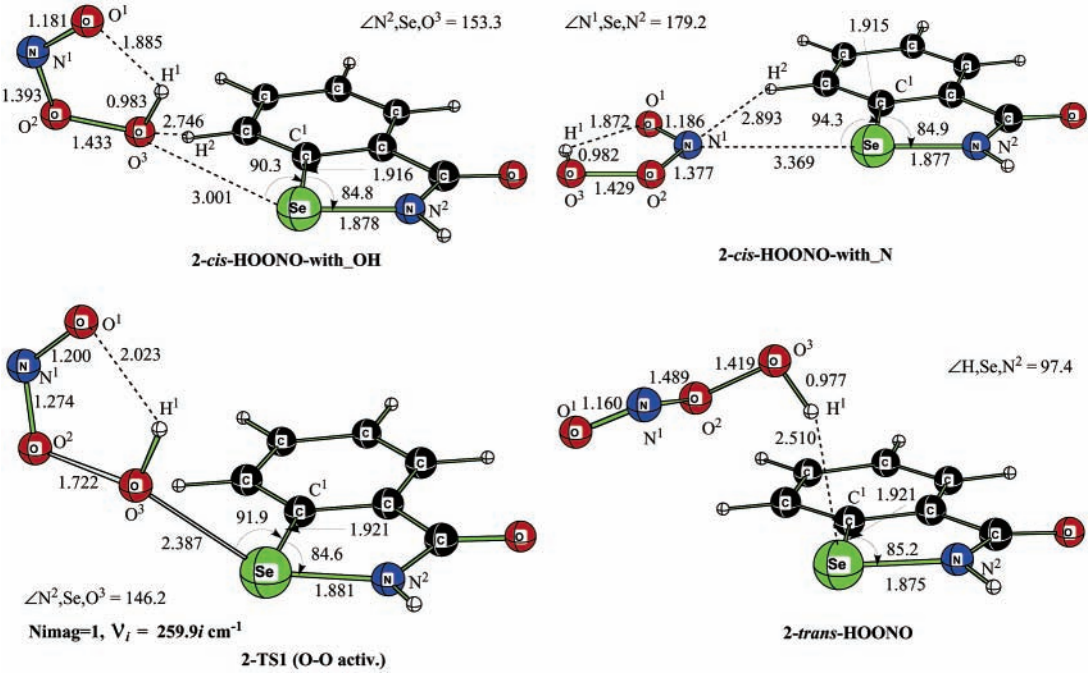

Figure 4. B3LYP/6-311G(d,p) calculated important geometries (distances in Å, angles in deg) of **2**−HOONO intermediate and O−O activation transition state, **2**−TS1, of the reaction of **2** with HOONO.

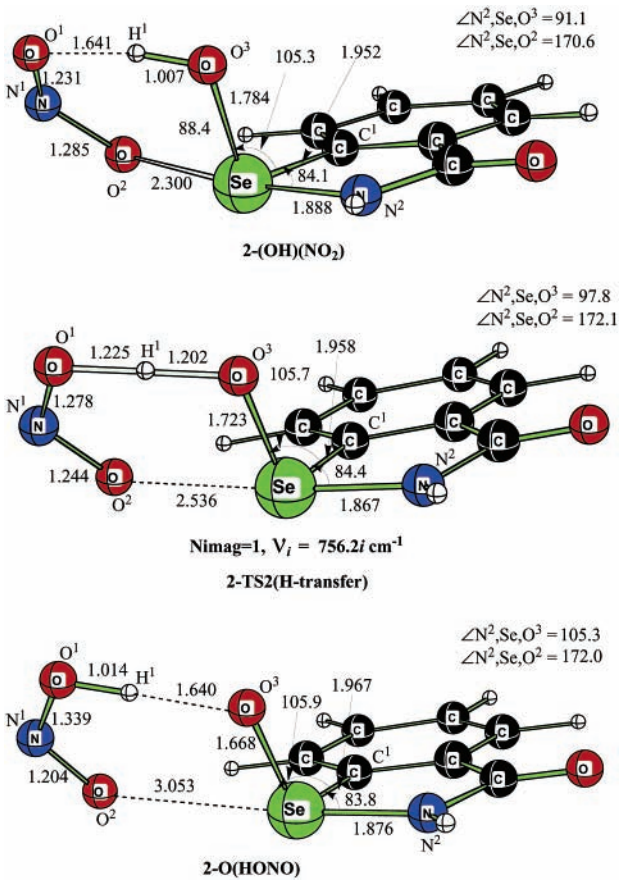

Figure 5. B3LYP/6-311G(d,p) calculated important geometrical parameters (distances in Å, angles in deg) of **2**−(OH)(NO_2) and **2**−O(HONO) intermediates, as well as **2**−TS2(H-transfer) transition state of the reaction of **2** with HOONO.

to the formation of the complex, **2**−(OH)(NO_2) (see Figure 5), where the Se−O^3H^1 bond is located out of the Se(C_6H_4CONH) plane with the ∠C^1SeO^3 and ∠N^2SeO^3 angles being 105.3 and 91.1°, respectively.

The calculated Se−O^3H^1 bond distance of 1.784 Å is significantly shorter (by 0.603 Å) than that in the **2**−TS1(O−O activ.) transition state. Interestingly, despite the formation of strong Se−O^3H^1 bond, the Se−N^2 bond distance in **2**−(OH)(NO_2) is almost the same as that in **2**−TS1(O−O activ.) or in the **2**−*cis*-HOONO_with_OH complex, indicating an insignificant cis effect between the Se−N^2 and Se−O^3 bonds. The calculated ∠N^2SeO^2 angle is 170.6°, indicating that the NO_2 group is bound to the Se-center trans to the Se−N^2 bond. The calculated Se−O^2 bond distance is 2.300 Å, indicating a weak Se−$O^2N^1O^1$ interaction energy. However, the O^1 end of the $O^2N^1O^1$ fragment involved a strong hydrogen bonding interaction with the H^1 atom of the O^3H^1-group. The calculated O^2−H^1 and O^3−H^1 bond distances are 1.641 and 1.007 Å, respectively. This H-bonding causes an elongation of the N^1−O^1 bond by 0.031 Å in **2**−(OH)(NO_2) compared to that in **2**−TS1(O−O activ.). In addition, we believe that the hydrogen bonding in O^2−H^1 is a major reason for the existence of the $O^2N^1O^1$ group in the coordination sphere of the Se-center.

The energetic data, given in Table 1, show that the product **2**−(OH)(NO_2) complex lies 34.8 (21.1) kcal/mol lower in energy than the reactants, *cis*-HOONO and **2**.

We are aware of the existence of other, energetically less favorable, isomers for complex **2**−(OH)(NO_2). However, the existence of these isomers does not make a significant contribution to the mechanism of the reaction of HOONO and **2** and, therefore, will not be discussed here.

Process Starting from the 2-(OH)(NO_2) Complex. From the **2**−(OH)(NO_2) complex, the reaction may split into two distinct channels: •NO_2 dissociation and formation of selenenic acid, **2**−OH•, and H-atom transfer from HOSe(C_6H_4CONH) to the NO_2 fragment to form HONO and selenoxide, **2**−O (see Figure 6). We will discuss these processes separately.

Our calculations show that •NO_2 dissociation from the complex **2**−(OH)(NO_2) occurs without any energy barrier and is endothermic by 24.7 (8.3) kcal/mol. Comparison of the values given with and without parenthesis shows that the entropy effect is very important. The inclusion of an entropy term in the

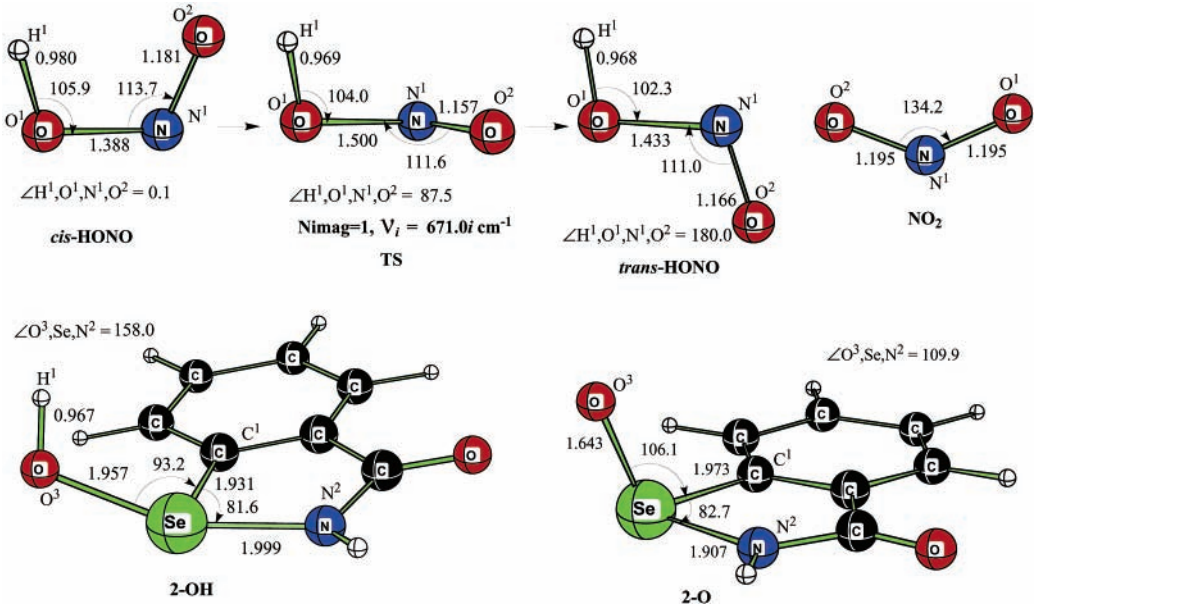

Figure 6. B3LYP/6-311G(d,p) calculated important geometrical parameters (distances in Å, angles in deg) of possible products of the reaction of **2** with HOONO.

calculations reduces the endothermicity of the reaction by 16.4 kcal/mol. The final products, **2**−OH• and •NO_2, lie 12.1(12.8) kcal/mol lower than the reactants, **2** and *cis*-HOONO.

However, the second process, starting form the same **2**−(OH)(NO_2) complex, involving an H-atom transfer from HOSe(C_6H_4CONH) to an NO_2 fragment, occurs with a small energy barrier (2.5 (0.3) kcal/mol) at the **2**−TS2(H-transfer) state and leads to formation of the **2**−O(HONO) complex (see Figure 5), which lies only 1.0(1.6) kcal/mol lower than for complex **2**−(OH)(NO_2).

As can be seen in Figure 5, the **2**−TS2(H-transfer) state is a real transition state, with a single imaginary frequency at 856.2i cm^{-1}, corresponding to an H^1-atom transfer from H^1OSe-(C_6H_4CONH) to an NO_2 fragment. Compared to complex **2**−(OH)(NO_2)**,** in this transition state, the Se−O^2 and O^3−H^1 bonds are elongated by 0.236 and 0.195 Å, but the O^1−H^1 and Se−O^3 bonds formed are shortened by 0.416 and 0.061 Å, respectively. The N^1−O^1 and N^1−O^2 bonds in the **2**−TS2(H-transfer) state are changed according to the nature of this process.

Overcoming the small H-atom transfer barrier leads to the formation of the **2**−O(HONO) complex (Figure 5), where the Se−O^2 bond (3.053 Å) is completely broken, but where O^1−H^1 and Se−O^3 bonds (1.014 and 1.668 Å, respectively) are formed. The HONO molecule formed is bound to an OSe(C_6H_4-CONH) fragment with an H^1−O^3 hydrogen bond of 1.640 Å in length.

The dissociation of the HONO molecule from **2**−O(HONO) is calculated to be endothermic by 10.5 kcal/mol at the Δ*E* level. However, the inclusion of entropy and zero-point energy corrections makes this process slightly more exothermic by 1.2 kcal/mol.

Nitrogen-containing adducts of the reaction, the •NO_2 radical and the HONO molecule, are given in Figure 6. As can be seen from this figure, HONO has two different isomers: cis and trans, which are separated by a transition state, TS, corresponding to a rotation around the HO−NO bond. The rotational angle in the TS was found to be 87.5°. The results given in Table 1 show that the *trans*-HONO molecule is slightly, by 1.1(1.1) kcal/mol, more stable than the *cis*-HONO molecule. The energy barrier separating these two isomers was calculated from the *cis*-HONO molecule to be 10.8 (10.4) kcal/mol.

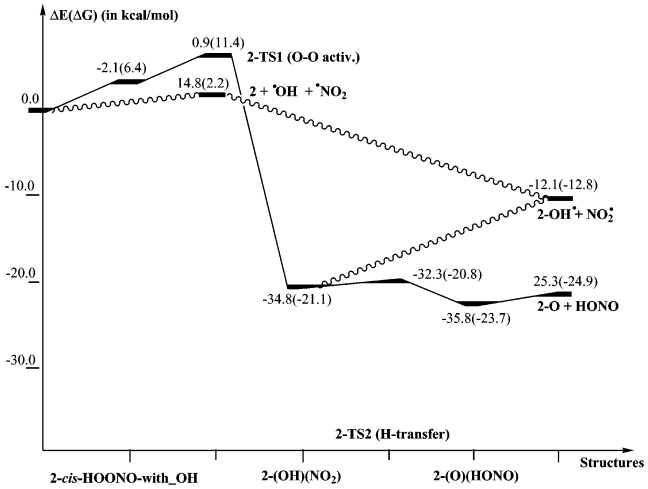

Figure 7. Schematic presentation (based on Δ*G* values) of potential energy profile of the reaction **2** with HOONO in the gas phase. Numbers presented here were calculated at the B3LYP/6-311+G(d,p)//B3LYP/6-311G(d,p) level. Numbers given without parenthesis are Δ*E* values, whereas those in parenthesis are ΔG values.

Overall Potential Energy Surface of the Reaction of 2 with *cis*-HOONO in the Gas Phase. The overall potential energy surface of the reaction of **2** with *cis*-HOONO in the gas phase is shown in Figure 7.

As can be seen from this figure, the reaction **2** + *cis*-HOONO → **2**−O + *cis*-HONO is exothermic in the gas phase with an energy of 25.3 (24.9) kcal/mol and may proceed via two different pathways: stepwise and concerted. The concerted pathway starts with O−O bond cleavage with an energy barrier of 0.9 (11.4) kcal/mol at the **2**−TS1(O−O activ.) transition state and leads to the **2**−(OH)(NO_2) intermediate. From the resultant complex, the reaction proceeds via an H-atom transfer from HOSe(C_6H_4CONH) to NO_2 and leads to the formation of *cis*-HONO and selenoxide, **2**−O. The H-atom transfer from HOSe(C_6H_4CONH) to NO_2 was calculated to be exothermic by 1.0 (2.6) kcal/mol and occurred with only a 2.5 (0.3) kcal/mol energy barrier.

TABLE 3: Calculated Relative Energies (kcal/mol) of the Reactants, Intermediates, Transition States, and Products of the Reaction of 2 with HOONO in the Gas Phase (at the B3LYP/6-311G(d,p)//B3LYP/6-311+G(d,p) Level) and Cyclohexane, Benzene, Dichloromethane, and Water (Calculated at the PCM-B3LYP/6-311+G(d,p)//B3LYP/6-311G(d,p) Level).

	gas phase		C_6H_{12}		C_6H_6		CH_2Cl_2		H_2O	
structures	ΔE	ΔG	ΔE	ΔG	ΔE	ΔG	ΔE	ΔG	ΔE	ΔG
HOONO										
cis	0.0	0.0	0.0	0.0	0.0	0.0	0.0	0.0	0.0	0.0
TS	13.4	12.5	13.1	12.2	13.1	12.2	12.0	11.1	9.8	8.9
trans	2.1	1.6	1.5	1.0	1.5	1.0	0.4	−0.1	−1.8	−2.3
HONO										
cis	0.0	0.0	0.0	0.0	0.0	0.0	0.0	0.0	0.0	0.0
TS	11.8	10.4	11.7	10.3	11.7	10.3	11.4	10.0	10.9	9.5
trans	−1.1	−1.1	−1.2	−1.2	−1.2	−1.2	−1.3	−1.3	−1.0	−1.0
2 + *cis*-HOONO	0.0	0.0	0.0	0.0	0.0	0.0	0.0	0.0	0.0	0.0
2−*cis*-HOONO-with_OH	−2.1	6.4	−0.1	8.4	−0.4	8.1	0.7	9.2	0.9	9.4
2−*cis*-HOONO-with_N	−0.8	7.3	1.1	9.2	0.9	9.0	1.6	9.7	2.5	10.6
2−*trans*-HOONO	−1.0	9.1	2.0	12.1	1.7	11.8	2.5	12.6	3.7	13.8
2−TS1 (O−O activ.)	0.9	11.4	2.6	13.1	2.4	12.9	3.3	13.8	3.9	14.4
2−(OH)(NO_2)	−34.8	−21.1	−34.9	−21.2	−35.2	−21.5	−34.9	−21.2	−34.9	−21.2
2−TS2 (H-transfer)	−32.3	−20.8	−32.4	−20.9	−32.8	−21.3	−32.5	−21.0	−32.6	−21.1
2−O(HONO)	−35.8	−23.7	−35.0	−22.9	−35.2	−23.1	−34.8	−22.7	−34.7	−22.6
2−O + HONO	−25.3	−24.9	−26.5	−26.1	−26.5	−26.1	−28.2	−27.8	−31.4	−31.0
2−OH + NO_2	−12.1	−12.8	−11.8	−12.5	−11.6	−12.3	−11.7	−12.4	−11.4	−12.1

The first step of the stepwise pathway is O−O bond homolysis in *cis*-HOONO, which occurs with an energy of 14.8 (2.2) kcal/mol, and leads to the formation of HO$^\bullet$ and ONO$^\bullet$ radical pairs. In the next step, the recombination of the HO$^\bullet$ radical with compound **2** occurs and leads to formation of selenenic acid, **2**−OH$^\bullet$. The **2**−OH$^\bullet$ and $^\bullet NO_2$ energies lie 12.1 (12.8) kcal/mol lower than the reactants, **2** and *cis*-HOONO. Later, the $^\bullet NO_2$ radical simultaneously coordinates with **2**−OH$^\bullet$, and this leads to formation of the **2**−(OH)(NO_2) complex, where the stepwise pathway merges with the concerted pathway described above.

A comparison of the concerted and stepwise mechanisms shows that the rate-limiting step of both mechanisms is the O−O bond utilization, which occurs much more easily for the concerted process at the ΔE and ΔE + ZPC (enthalpy) levels. However, including entropy corrections alters the positions of the **2**−TS1(O−O activ.) transition state and the **2** + $^\bullet$OH + $^\bullet NO_2$ dissociation limit on the energy scale, and this makes the stepwise mechanism more favorable in the gas phase.

In either case, the only selenium-containing product of the reaction of compound **2** (and ebselen) with *cis*-HOONO is going to be selenoxide, which is in agreement with the available experimental data.[20,21]

IV. Role of the Solvent

The effects of the solvent were taken into consideration at the PCM-B3LYP/6-311+G(d,p) level using the B3LYP/6-311G(d.p) optimized geometries. Here, we used water, dichloromethane, benzene, and cyclohexane as the solvent. Their dielectric constants were taken from the Gaussian98 quantum chemical package.[23] Note that the single point PCM calculations provide a value called the ΔG(solution), which does not include the zero-point energy and entropy corrections, $\Delta\Delta$, and can be compared only with the ΔE value from the gas phase. Therefore, we will denote this value by ΔE solution. To include the zero-point energy and entropy corrections, one has to optimize the geometries and recalculate the frequencies of each structure in the solution phase. However, these calculations were not performed as part of this work, and therefore, we calculated $\Delta\Delta$ in the gas phase and added it to deltaG (solution). The final quantity was called ΔG, because it included the zero-point energy and entropy corrections.

In Table 3 we show the calculated relative energies of the important points of the potential energy surface of the reaction of **2** with HOONO.

As seen from this table, the inclusion of solvent effects slightly increases the rate-determining O−O bond utilization barriers for both the concerted and stepwise pathways. For the concerted pathway, the O−O bond cleavage barrier at the **2**−TS1(O−O activ.) transition state, which was calculated to be 0.9 (11.4) kcal/mol in the gas phase, becomes 2.6 (13.1), 2.4 (12.9), 3.3 (13.8), and 3.9 (14.4) kcal/mol in cyclohexane, benzene, dichloromethane, and water, respectively. In addition, the ΔE value of the O−O bond homolysis in *cis*-HOONO, which was 14.8 kcal/mol in the gas phase, becomes 14.9, 14.0, 15.2, and 13.5 kcal/mol in cyclohexane, dichloromethane, benzene, and water, respectively. The inclusion of solvent effects only slightly changes the other calculated gas-phase energies.

Thus, the ΔE values for the rate-determining O−O bond utilization step of the concerted and stepwise mechanisms are 2.6, 2.4, 3.3, and 3.9 kcal/mol, and 14.9, 14.0, 15.2, and 13.5 kcal/mol, in cyclohexane, benzene, dichloromethane, and water, respectively. A comparison of these data indicates that *even in solution, the reaction of compound 2 with HOONO prefers to proceed via the concerted mechanism.* Because we did not explicitly calculate the entropy effects in solution, which can be dramatically different in the gas and solution phases, here, we prefer to discuss only the ΔE values of the concerted and stepwise pathways. Because the energy difference between the rate-determining barriers of the concerted and stepwise mechanisms is large (10 kcal/mol or more), we do not expect that the inclusion of the entropy effects in solution (which are expected to be only a few kcal/mol) will greatly change our ΔE-based conclusions.

V. Comparison of the Reaction Mechanisms of Ebselen (Compound 2) with ONOO− and HOONO

We will now compare the calculated mechanisms of the reactions of compound **2** with $ONOO^-$ and HOONO.

As has been discussed,[22] the reaction of **2** with $ONOO^-$ (below called PN) proceeds via the following pathway: **2** + PN → **2**−PN → **2**−TS1 (O−O activ.) → **2**−(O)(NO_2^-) → **2**−O + NO_2^-. In the gas phase, the first step of the reaction, the formation of **2**−*cis*-PN, is highly exothermic, with an energy

of 32.2 (20.9) kcal/mol. The O−O activation barrier is only 7.1 (7.7) kcal/mol relative to the pre-reaction complex, **2**−*cis*-PN. *More importantly, the transition state corresponding to the O−O bond cleavage lies about 25.1 (13.2) kcal/mol lower than the reactants, indicating that the O−O activation process should occur extremely fast in the gas phase.* The rate-determining 26.4 (14.8) kcal/mol barrier for this reaction corresponds to the dissociation energy of NO_2^-, which is the final step of the reaction. The entire reaction is exothermic with an energy of 31.6 (31.2) kcal/mol.

However, in the gas phase, the rate-determining step of the reaction of compound **2** with HOONO is the O−O bond utilization step, for both the concerted and stepwise mechanisms. The transition state, **2**−TS1(O−O activ.), and O−O bond homolysis corresponding to the concerted and stepwise pathways lie 0.9 (11.4) and 14.8 (2.2) kcal/mol *higher* than the reactants, respectively. A comparison of these data for HOONO and $ONOO^-$ indicate that, *in the gas phase, the transition states corresponding to the O−O bond cleavage lies lower than the reactants for the reaction with* $ONOO^-$*, but higher than the reactants for the reaction with HOONO. As a result, the reaction of compound* ***2*** *(and ebselen) with HOONO is significantly slower than that of compound* ***2*** *(and ebselen) with* $ONOO^-$. Although the final selenium-containing products of both reactions are going to be selenoxide, the reaction of **2** with $ONOO^-$ in the gas phase may also produce the O−O bond cleavage complex, **2**−(O)(NO_2^-).

The inclusion of solvent effects changes the rate-determining step of the reaction of **2** with $ONOO^-$ from NO_2^- dissociation to an O−O cleavage step, which is calculated to occur with energy barriers of 8.3 (13.9), 7.8 (8.4), 7.8 (8.4), and 7.6 (8.2) kcal/mol in water, dichloromethane, benzene, and cyclohexane, respectively. Importantly, in water, the transition state for O−O activation is calculated to be 2.0 kcal/mol higher than the reactants. However, in relatively nonpolar solvents, such as dichloromethane, benzene, and cyclohexane, it is still lower in energy than the reactants by 4.4, 12.2, and 13.0 kcal/mol, respectively. For the reaction of **2** with HOONO, inclusion of the solvent effect does not change the conclusion derived from the gas phase studies. It only slightly increases the rate-determining O−O cleavage energy barrier calculated from the reactants: from 0.9 kcal/mol in the gas phase to 3.9 (14.4), 3.3 (13.8), 2.4 (12.9), and 2.6 (13.1) in water, dichloromethane, benzene, and cyclohexane, respectively. Comparison of these data for the reaction of **2** with $ONOO^-$ and HOONO indicates that *even in solution, the reaction of* ***2*** *(and ebselen) with HOONO should be slower than that with* $ONOO^-$*, especially in nonpolar solvents. The only selenium-containing product of both reactions is going to be selenoxide.* All the conclusions derived in the present paper are in good agreement with available experimental data.[20,21]

It is noteworthy that the reaction of **2** with peroxynitrite anion is found to be a two-electron oxidation process and occurs via a heterolytic O−O bond cleavage, whereas the reaction of **2** with HOONO is found to be a one-electron oxidation process and occurs via a homolytic O−O bond cleavage.

Thus, our data clearly show that the observed[20] lower yield of selenoxide at high pH values is partially due to the large O−O bond cleavage barrier for HOONO compared to $ONOO^-$, which is caused by a weaker ebselen−HOONO interaction than an ebselen−$ONOO^-$ interaction.

VI. Conclusions

From the above presented discussions we can deduce the following conclusions.

1. The B3LYP and CCSD(T) calculations with numerous basis sets show that the B3LYP method is not a reliable method for studying the energetics and stability of the weakly bound $^{\bullet}OH\cdots ONO^{\bullet}$ structure and may lead to the wrong conclusions.

2. The CCSD(T) calculations with the 6-311+G(d,p) and 6-311+G(3df,2p) basis sets (after including the zero-point energy and entropy corrections) indicate that the $^{\bullet}OH\cdots ONO^{\bullet}$ structure is unlikely to exist in the gas phase. Furthermore, the inclusion of solvent (water) molecules in the calculations resulted in a complete cleavage of the weak interaction between the $^{\bullet}OH$ and $ONO^{\bullet}$ radicals in $^{\bullet}OH\cdots ONO^{\bullet}$. Therefore, it is predicted that in solution, the reaction mechanism of HOONO with antioxidants, if it proceeds via O−O homolysis, should resemble that for a solvated $^{\bullet}OH$ radical, at least in polar solvents, such as water.

3. The reaction **2** + *cis*-HOONO → **2**−O + *cis*-HONO was found to be exothermic in the gas phase with an energy of 25.3 (24.9) kcal/mol; it can proceed via two different pathways: stepwise and concerted. Among these two, the concerted pathway proceeds via an O−O bond cleavage transition state, **2**-TS2(O−O activ.), which is more favorable at the enthalpy level. However, on including an entropy correction, the stepwise mechanism via an O−O bond homolysis in *cis*-HOONO is more favorable in the gas phase. The only selenium-containing product of the reaction of ebselen with HOONO is predicted to be selenoxide, which is in agreement with the available experimental data.[20,21]

4. The inclusion of solvent effects only slightly increases the rate-determining O−O bond cleavage energy barrier and the O−O bond homolysis energy for the concerted and stepwise mechanisms, respectively. Comparison of the calculated enthalpy data indicates that *even in solution, the reaction of compound* ***2*** *(and ebselen) with HOONO prefers to proceed via a concerted mechanism.*

5. A comparison of the energetics of the reactants, intermediates, and transition states of the reaction of **2** with *cis*-HOONO and *cis*-$ONOO^-$ shows that, in both the gas phase and in solution, the reaction of **2** (and ebselen) with HOONO is significantly slower than that of **2** (and ebselen) with $ONOO^-$. Our data clearly show that the observed[20] lower yield of selenoxide at high pH values is partially due to the larger O−O bond cleavage barrier for HOONO than for $ONOO^-$ and is caused by a weaker ebselen−HOONO interaction compared to an ebselen−$ONOO^-$ interaction.

6. It is noteworthy that the reaction of **2** with peroxynitrite anion is a two-electron oxidation process and occurs via a heterolytic O−O bond cleavage, whereas the reaction of **2** with HOONO is a one-electron oxidation process and occurs via homolytic O−O bond cleavage.

Acknowledgment. D.G.M. acknowledges the Visiting Professorship awarded by the University of Tokyo and thanks Dr. Yu. V. Geletii for multiple discussions on the problems of peroxynitrite chemistry. Acknowledgment is also made to the Cherry L. Emerson Center of Emory University for the use of its resources, which are in part supported by a National Science Foundation grant (CHE-0079627) and an IBM Shared University Research Award.

Supporting Information Available: The Cartesian coordinates of all calculated reactants, intermediates, transition states, and products of the reaction of **2** and HOONO (Table S1), their total energies (Table S2), Mulliken charges (Table S3), Cartesian coordinates of the $(H_2O)_n(^{\bullet}OH\cdots ONO^{\bullet})$ complexes (for $n = 0$, 1, and 2) (Table S4), their B3LYP and CCSD(T) energies (Table

S5), and the calculated ΔG(solvation) values at the PCM level for all the reactants, intermediates, transition states, and products of the reaction of **2** with HOONO (Table S6) are available free of charge via the Internet at http://pubs.acs.org.

References and Notes

(1) See: (a) Beckman, J. S.; Beckman, T. W.; Chen, J.; Marshall, P. A.; Freeman, B. A. *Proc. Acad. Sci. U.S.A.* **1990**, *87*, 1620. (b) Beckman, J. S.; Crow, J. P. *Biochem. Soc. Transact.* **1993**, *21*, 330. (c) Ischiropoulos, H.; Zhu, L.; Beckman, J. S. *Arch. Biochem. Biophys.* **1992**, *298*, 446. (d) Huie, R. E.; Padmaja, S. *Free Radical Res. Commun.* **1993**, *18*, 195. (e) Beckman, J. S. The Physiological and Pathophysiological Chemistry of Nitric Oxide. In *Nitric Oxide: Principles and Actions*; Lancaster, J., Ed.; Academic Press: San Diego, CA, 1996; p 1.

(2) (a) Koppenol, W. H.; Moreno, J. J.; Pryor, W. A.; Ischiropoulos, H.; Beckman, J. S. *Chem. Res. Toxicol.* **1992**, *5*, 834. (b) Kissner, R.; Nauser, T.; Bugnon, P.; Lyle, P. G.; Koppenol, W. H. *Chem. Res. Toxicol.* **1998**, *11*, 557.

(3) Pryor, W. A.; Gueto, R.; Jin, X.; Koppenol, W. H.; Ngu-Schwemlein, M.; Squadrito, G. L.; Uppu, P. L.; Uppu, R. M. *Free Radical Biol. Med.* **1995**, *18*, 75.

(4) Rosen, G. M.; Freeman, B. A. *Proc. Acad. Sci. U.S.A.* **1984**, *81*, 7269.

(5) Marla, S. S.; Lee, J.; Groves, J. T. *Proc. Acad. Sci. U.S.A.* **1997**, *94*, 14243.

(6) Denicola, A.; Souza, J. M.; Radi, R. *Proc. Acad. Sci. U.S.A.* **1998**, *95*, 3566.

(7) Rachmilewitz, D.; Stamler, J. S.; Karmeli, F.; Mullins, M. E.; Singel, D. J.; Loscalzo, J.; Xavier, R. J.; Podolsky, D. K. *Gastroenterology* **1993**, *105*, 1681.

(8) Squadrito, G. L.; Jin. X.; Pryor, W. A. *Arch. Biochem. Biophys.* **1995**, *322*, 53.

(9) Lee, J.; Hunt, J. A.; Groves, J. T. *J. Am. Chem. Soc.* **1998**, *120*, 6053.

(10) Crow, J. P.; Beckman, J. S.; McCord, J. M. *Biochemistry* **1995**, *43*, 3544.

(11) Gatti, R. M.; Radi, R.; Augusto, O. *FEBS Lett*. **1994**, *348*, 287.

(12) Szabo, C.; Ohshima, H. *Nitric Oxide: Biol. Chem.* **1997**, *1*, 373.

(13) (a) Stern, M. K.; Jensen, M. P.; Kramer, K. *J. Am. Chem. Soc.* **1996**, *118*, 8735. (b) Crow, J. P. *Arch. Biochem. Biophys.* **1999**, *371*, 41. (c) Lee, J.; Hunt, J. A.; Groves, J. T. *Bioorg. Med. Chem. Lett.* **1997**, *7*, 2913. (d) Hunt, J. A.; Lee, J.; Groves, J. T. *Chem. Biol.* **1997**, *4*, 845. (e) Crow, J. P. *Free Radical Biol. Med.* **2000**, *28*, 1487. (f) Balavoine, G. G. A.; Geletti, Y. V.; Bejan, D. *Nitric Oxide: Biol. Chem.* **1997**, *1*, 507. (g) Shimanovich, R.; Hannah, S.; Lynch, V.; Gerasimchuk, N.; Mody, T. D.; Magda, D.; Sessler, J.; Groves, J. T. *J. Am. Chem. Soc.* **2001**, *123*, 3613. (h) Zhang, X.; Busch, D. H. *J. Am. Chem. Soc.* **2000**, *122*, 1229. (i) Salvemini, D.; Wang, Z. Q.; Stern, M.; Currie, M. G.; Misko, T. *Proc. Natl. Acad. U.S.A.* **1998**, *95*, 2659.

(14) See: Jensen, M. P.; Riley, D. P. *Inorg. Chem.* **2002**, *41*, 4788 and references therein.

(15) (a) Floris, R.; Piersma, S. R.; Yang, G.; Jones, P.; Wever, R. *Eur. J. Biochem.* **1993**, *215*, 767. (b) Kondo, H.; Takahashi, M.; Niki, E. *FEBS Lett.* **1997**, *413*, 236. (c) Exner, M.; Herold, S. *Chem. Res. Toxicol.* **2000**, *13*, 287. (d) Squadrito, G. L.; Pryor, W. A. *Chem. Res. Toxicol.* **1997**, *11*, 7718. (e) Radi, R. *Chem. Res. Toxicol.* **1998**, *11*, 720. (f) Minetti, M.; Scorza, G.; Pietraforte, D. *Biochemistry* **1999**, *38*, 2078. (g) Herold, S.; Matsui, T.; Watanabe, Y. *J. Am. Chem. Soc.* **2001**, *123*, 4085. (h) Bourassa, J. L.; Ives, E. P.; Marqueling, A. L.; Shimanovich, R.; Groves, J. T. *J. Am. Chem. Soc.* **2001**, *123*, 5142.

(16) *Selenium in Biology and Human Health*; Burk, R. F., Ed.; Springer-Verlag: New York, 1994 and references therein.

(17) (a) Mugesh, G.; Singh, H. B. *Chem. Soc. Rev.* **2000**, *29*, 347. (b) Mugesh, G.; Panda, A.; Singh, H. B.; Punekar, N. S.; Butcher, R. J. *J. Am. Chem. Soc.* **2001**, *123*, 839. (c) Mugesh, G.; du Mont W. W.; Sies, H. *Chem. Rev.* **2001**, *101*, 2125 and references therein. (d) Briviba, K.; Roussyn, I.; Sharov, V. S.; Sies, H. *Biochem. J.* **1996**, *319*, 13.

(18) Sies, H.; Masumoto, H. *Adv. Pharmacol.* **1997**, *38*, 2229 and references therein

(19) Perrin, D.; Koppenel, W. H. *Arch. Biochem. Biophys.* **2000**, *377*, 266.

(20) Masumoto, H.; Kissner, R.; Koppenol, W. H.; Sies, H. *FEBS Lett.* **1996**, *398*, 179.

(21) Masumoto, H.; Sies, H. *Chem. Res. Toxicol.* **1996**, *9*, 262.

(22) Musaev, D. G.; Geletii, Yu. V.; Hill, C. L.; Hirao, K. *J. Am. Chem. Soc.*, in press.

(23) Frisch, M. J.; Trucks, G. W.; Schlegel, H. B.; Scuseria, G. E.; Robb, M. A.; Cheeseman, J. R.; Zakrzewski, V. G.; Montgomery, J. A., Jr.; Stratmann, R. E.; Burant, J. C.; Dapprich, S.; Millam, J. M.; Daniels, A. D.; Kudin, K. N.; Strain, M. C.; Farkas, O.; Tomasi, J.; Barone, V.; Cossi, M.; Cammi, R.; Mennucci, B.; Pomelli, C.; Adamo, C.; Clifford, S.; Ochterski, J.; Petersson, G. A.; Ayala, P. Y.; Cui, Q.; Morokuma, K.; Malick, D. K.; Rabuck, A. D.; Raghavachari, K.; Foresman, J. B.; Cioslowski, J.; Ortiz, J. V.; Baboul, A. G.; Stefanov, B. B.; Liu, G.; Liashenko, A.; Piskorz, P.; Komaromi, I.; Gomperts, R.; Martin, R. L.; Fox, D. J.; Keith, T.; Al-Laham, M. A.; Peng, C. Y.; Nanayakkara, A.; Gonzalez, C.; Challacombe, M.; Gill, P. M. W.; Johnson, B.; Chen, W.; Wong, M. W.; Andres, J. L.; Gonzalez, C.; Head-Gordon, M.; Replogle, E. S.; Pople, J. A. *Gaussian 98*, Revision A.7; Gaussian, Inc.: Pittsburgh, PA, 1998.

(24) (a) Becke, A. D. *Phys. Rev. A* **1988**, *38*, 3098. (b) Lee, C.; Yang, W.; Parr, R. G. *Phys. Rev. B* **1988**, *37*, 785. (c) Becke, A. D. *J. Chem. Phys.* **1993**, *98*, 5648.

(25) (a) Tsai, H. H.; Hamilton, T. P.; Tsai, J. H. M.; Van der Woerd, M.; Harrison, J. G.; Jablonsky, M. J.; Beckman, J. S.; Koppenol, W. H. *J. Phys. Chem.*, **1996**, *100*, 15087. (b) Tsai, J. H. M.; Harrison, J. G.; Martin, J. C.; Hamilton, T. P.; Van der Woerd, M.; Jablonsky, M. J.; Beckman, J. S. *J. Am. Chem. Soc.* **1994**, *116*, 4115.

(26) McKee, M. L. *J. Am. Chem. Soc.* **1995**, *117*, 1629.

(27) Bach, R. D.; Glukhovtsev, M. N.; Canepa, C. *J. Am. Chem. Soc.* **1998**, *120*, 775

(28) (a) Miertus, S.; Scrocco, E.; Tomasi, J. *Chem. Phys.* **1981**, *55*, 117. (b) Miertus, S.; Tomasi, J. *Chem. Phys.* **1982**, *65*, 239. (c) Cossi, M.; Barone, V.; Cammi, R.; Tomasi, J. *Chem. Phys. Lett.* **1996**, *255*, 327. (d) Cances, M. T.; Mennucci, V.; Tomasi, J. *J. Chem. Phys.* **1997**, *107*, 3032. (e) Barone, V.; Cossi, M.; Tomasi, J. *J. Comput. Chem.* **1998**, *19*, 404.

(29) (a) Shen, M.; Xie, Y.; Schaefer, H. F., III; Deakyne, C. A. *J. Chem. Phys.* **1990**, *93*, 3379. (b) McGrath, M. P.; Francl, M. M.; Rowland, F. S.; Hehre, W. J. *J. Phys. Chem.* **1988**, *92*, 5352. (c) Cheng, B.-M.; Lee, J.-W.; Lee, Y.-P. *J. Phys. Chem.* **1991**, *95*, 2814. (d) Koppenol, W. H.; Klasinc, L. *Int. J. Quantum Chem. Symp.* **1993**, *20*, 1. (e) McGrath, M. P.; Rowland, F. S. J. *J. Phys. Chem.* **1994**, *101*, 5494.

(30) Nagy, P. I. *J. Phys. Chem. A* **2002**, *106*, 2659.

(31) Pryor, W. A.; Squadrito, G. L. *Am. J. Physiol.* **1995**, *268*, L699.

(32) Koppenol, W. H.; Moreno, J. J.; Pryor, W. A.; Ischiropoulos, H.; Beckman, J. S. *Chem. Res. Toxicol.* **1992**, *5*, 834.

(33) See, Bartberger, M. D.; Olson, L. P.; Houk, K. N. *Chem. Res. Toxicol.* **1998**, *11*, 710 and references therein.

(34) (a) Cameron, D. R.; Borrajo, A. M. P.; Bennett, B. M.; Thatcher, G. R. J. *Can. J. Chem.* **1995**, *73*, 1627. (b) Jursic, B. S.; Klasinc, L.; Pecur, S.; Pryor, W. A. *Nitric Oxide: Biol. Chem.* **1997**, *1*, 494. (c) Sumathi, R.; Peyerimhoff, S. D. *J. Chem. Phys.* **1997**, *107*, 1872.

(35) (a) Houk, K. N.; Condroski, K. R.; Pryor, W. A. *J. Am. Chem. Soc.* **1996**, *118*, 13002. (b) Houk, K. N.; Liu, J.; DeMello, N. C.; Condroski, K. R. *J. Am. Chem. Soc.* **1997**, *119*, 10147.

(36) (a) Rappe, A. K.; Bernstein, E. R. J. *Phys. Chem. A* **2000**, *113*, 6117. (b) See Hobza, P.; Sponer J. *Chem. Rev.* **1999**, *99*, 3247 and references therein, (c) Sponer, J.; Leszczynski, J.; Hobza, P. J. *Phys. Chem. A* **1997**, *101*, 9489. (d) Sponer, J.; Hobza, P. *Chem. Phys. Lett.* **1997**, *267*, 263. (e) Kamiya, M.; Tsuneda, T.; Hirao, K. *J. Chem. Phys.* **2002**, *117*, 6010.

(37) Krauss, M. *Chem. Phys. Lett.* **1994**, *222*, 513.

(38) See: (a) Uppu, R. M.; Squadrito, G. L.; Pryor, W. A. *Arch. Biochem. Biophys.* **1996**, *327*, 335. (b) Uppu, R. M.; Winston, G. W.; Pryor, W. A. *Chem. Res. Toxicol.* **1997**, *10*, 1331 and references therein.

(39) Pryor, W. A.; Jin, X.; Squadrito, G. L. *Proc. Natl. Acad. Sci. U.S.A.* **1994**, *91*, 11173.

(40) (a) Gonzalez, C.; Schlegel, H. B. *J. Chem. Phys.* **1989**, *90*, 2154. (b) Gonzalez, C.; Schlegel, H. B. *J. Phys. Chem.* **1990**, *94*, 5523.